MOLECULAR AND CELLULAR BIOLOGY, Jan. 2008, p. 258–268 Vol. 28, No. 1
0270-7306/08/$08.00+0 doi:10.1128/MCB.01536-07

p27^{kip1} Deficiency Impairs G_2/M Arrest in Response to DNA Damage, Leading to an Increase in Genetic Instability▽

Shannon R. Payne,[1]† Shulin Zhang,[2] Karen Tsuchiya,[1] Russell Moser,[1] Kay E. Gurley,[1] Gary Longton,[1] Johan deBoer,[2] and Christopher J. Kemp[1]*

Fred Hutchinson Cancer Research Center, Seattle, Washington,[1] and University of Victoria, Victoria, British Columbia, Canada[2]

Received 22 August 2007/Returned for modification 19 September 2007/Accepted 9 October 2007

p27^{kip1} is a cyclin-dependent kinase inhibitor and a tumor suppressor. In some tumors, p27 suppresses tumor growth by inhibition of cell proliferation. However, this is not universally observed, implying additional mechanisms of tumor suppression by p27. *p27*-deficient mice are particularly susceptibility to genotoxin-induced tumors, suggesting a role for p27 in the DNA damage response. To test this hypothesis, we measured genotoxin-induced mutations and chromosome damage in *p27*-deficient mice. Both $p27^{+/-}$ and $p27^{-/-}$ mice displayed a higher *N*-ethyl-*N*-nitrosourea-induced mutation frequency in the colon than $p27^{+/+}$ littermates. Furthermore, cells from irradiated *p27*-deficient mice exhibited a higher number of chromatid breaks and showed modestly increased micronucleus formation compared to cells from wild-type littermates. To determine if this mutator phenotype was related to the cell cycle-inhibitory function of p27, we measured cell cycle arrest in response to DNA damage. Both normal and tumor cells from *p27*-deficient mice showed impaired G_2/M arrest following low doses of ionizing radiation. Thus, p27 may inhibit tumor development through two mechanisms. The first is by reducing the proliferation of cells that have already sustained an oncogenic lesion. The second is by transient inhibition of cell cycle progression following genotoxic insult, thereby minimizing chromosome damage and fixation of mutations.

Levels of p27 protein have prognostic significance in a wide variety of human cancers (reviewed in references 29 and 43). Decreased levels of p27 are associated with high tumor grade and stage in human colorectal (8, 37), gastric (48), breast (5, 15), and other cancers. Reduction of p27 protein in tumors correlates significantly with decreased survival in colorectal (18), gastric (20), breast (32), and esophageal squamous cell (38) carcinoma patients, among others. This is in contrast to other cyclin-dependent kinase (CDK) inhibitors such as p21 and p18, for which prognostic significance is limited (reviewed in reference 43), leading us to question the specific role of p27 in tumor suppression.

These observations hinted that p27 plays a fundamental role in tumor suppression, although a cause-and-effect relationship was difficult to establish because somatic mutations in the *CDKN1B* gene, encoding p27, are rare in tumors (16, 30, 31). Studies of the p27 knockout mouse clearly showed that p27 is a potent tumor suppressor in multiple tissues, with a particularly strong effect within the gastrointestinal (GI) tract. Although spontaneous GI tumors are rare in *p27*-deficient mice fed a standard diet, these mice are highly predisposed to adenomas and adenocarcinomas throughout the small intestine and colon when treated with the genotoxic carcinogens *N*-ethyl-*N*-nitrosourea (ENU), gamma irradiation, and 1,2-dimethylhydrazine (12, 28, 47).

Two primary, and sometimes overlapping, functions of tumor suppressors are inhibition of proliferation and maintenance of genetic integrity. Previously, we demonstrated that *p27* deficiency resulted in an increased mitotic index (MI) in GI tumors (28), indicating that p27 functions, at least in part, to inhibit proliferation of tumor cells. However, other studies show a lack of correlation between p27 levels and proliferation, suggesting that there may be more than one mechanism of tumor suppression by p27 (24, 25, 39, 42). Here we investigated the role of p27 in maintenance of genetic integrity using the same target tissue, the GI tract, and the same agents, ENU and gamma radiation, used previously to induce tumors.

We found that *p27* deficiency significantly increased both large- and small-scale genetic lesions in response to ENU and low doses of gamma irradiation using three separate genotoxic assays (the Big Blue mutagenicity assay, analysis of chromatid gaps and breaks, and the micronucleus assay). *p27* deficiency also impaired G_2/M arrest in the crypt progenitor cells of the GI epithelium following genotoxic exposure. Together, these results suggest that the susceptibility of *p27*-deficient mice to genotoxic agents can be at least partially attributed to an increase in genotoxin-induced mutation frequency (MF) due to a defect in G_2/M checkpoint initiation.

MATERIALS AND METHODS

Mice. Mixed 129/Sv × C57BL/6 *p27*-deficient mice were obtained from J. Roberts and genotyped as described previously (13). The *p27* knockout allele was backcrossed 14 times onto the C57BL/6 strain. For analysis of the in vivo MI, mice at the age of 8 to 12 weeks were treated with a single dose of whole-body ionizing radiation (IR) (with a ^{137}C source at 330 cGy per second). Six $p27^{+/+}$, five $p27^{+/-}$, and four $p27^{-/-}$ mice were treated with 0 Gy; four $p27^{+/+}$, four $p27^{+/-}$, and six $p27^{-/-}$ mice were treated with 0.6 Gy; eight $p27^{+/+}$, five $p27^{+/-}$, and five $p27^{-/-}$ mice were treated with 1.2 Gy; and four $p27^{+/+}$, four $p27^{+/-}$, and four $p27^{-/-}$ mice were treated with 4 Gy. For analysis of MI in tumor-bearing mice, the *p27* knockout allele was crossed to C57BL/6 Apc^{1638N} (14) or C3H Apc^{min} strains. When mice developed intestinal tumors, they were irradiated and sacrificed 2 to 4 h later. Eight $p27^{+/+}$, eight $p27^{+/-}$, and five $p27^{-/-}$ mice were

* Corresponding author. Mailing address: Fred Hutchinson Cancer Research Center C1-015, 1100 Fairview Ave. N., Seattle, WA 90109-1024. Phone: (206) 667-4252. Fax: (206) 667-5815. E-mail: cjkemp@fhcrc.org.
† Present address: Epigenomics, Inc., Seattle, WA.
▽ Published ahead of print on 22 October 2007.

TABLE 1. MF in control and ENU-treated groups

Genotype	Control				ENU treatment			
	Mouse	PFU (10^5)	No. of mutants[a]	MF (10^{-5})	Mouse	PFU (10^5)	No. of mutants	MF (10^{-5})
$p27^{+/+}$	1	3.61	13	3.6	1	3.63	159	43.8
	2	3.80	19	5.0	2	2.61	104	39.8
	3	2.88	15	5.2	3	3.91	203	51.9
	4	3.02	10	3.3	4	3.37	178	52.8
	5	2.88	11	3.8	5	2.62	167	63.6
	6	2.31	10	4.3	6	1.73	100	57.9
	7	3.25	15	4.6				
	Mean ± SEM			4.3 ± 0.3				51.0 ± 3.3
$p27^{+/-}$	1	5.68	23	4.1	1	4.36	253	58.1
	2	3.42	14	4.1	2	2.88	180	62.6
	3	2.72	14	5.1	3	4.35	253	58.2
	4	2.69	11	4.1	4	3.02	197	65.2
	5	3.01	8	2.7	5	3.55	250	70.5
	6	3.05	11	3.6	6	2.62	176	67.1
	7	3.45	10	2.9				
	Mean ± SEM			3.8 ± 0.3				63.0 ± 2.0
$p27^{-/-}$	1	2.04	19	4.4	1	1.88	223	118.3
	2	2.52	7	2.8	2	1.97	186	94.6
	3	1.21	3	2.5	3	2.13	255	119.9
	4	2.46	24	9.8	4	2.28	284	124.8
	5	2.08	9	4.3	5	2.57	321	124.9
	6	2.38	11	4.6				
	7	2.20	13	5.9				
	Mean ± SEM			5.1 ± 1.0				117.3 ± 4.7

[a] The number of mutants is corrected for potential clonal expansion.

treated with 0 Gy; two $p27^{+/+}$, two $p27^{+/-}$, and two $p27^{-/-}$ mice were treated with 1.2 Gy; and two $p27^{+/+}$, two $p27^{+/-}$, and one $p27^{-/-}$ mice were treated with 3 Gy. Five to 23 tumors per genotype per irradiation dose were examined, with the exception of $p27^{-/-}$ mice irradiated with 3 Gy, where only two tumors were available for examination. Mitotic figures and apoptotic bodies were counted from at least 5,000 to 25,000 tumor cells or 75 crypts in formalin-fixed, hematoxylin-eosin (H&E)-stained sections at a final magnification of ×600. All experiments were approved by the IACUC and performed in accordance with the relevant guidelines and regulations.

Somatic mutation assay. The p27/*lacI* double-transgenic mice were generated by crossing Big Blue/*lacI* transgenic C57BL/6 mice and $p27^{+/-}$ C57BL/6 mice. The resulting $p27^{+/+}$, $p27^{+/-}$, and $p27^{-/-}$ *lacI* mice were genotyped as previously described (13, 23). Five to seven mice were assigned to each treatment group. At the age of 7 to 9 weeks, mice were treated with ENU (Sigma-Aldrich Co.) at a dose of 150 mg/kg (dissolved in 66.7 mM phosphate-buffered saline [PBS] solution) by a single intraperitoneal injection. Control mice were injected with PBS solution only. Three weeks after ENU treatment, the mice were sacrificed and colons were excised, rinsed with sterile PBS, flash frozen in liquid nitrogen, and stored at −80°C until needed. Genomic DNA was isolated as previously described (41). *lacI* transgenes were recovered from purified mouse chromosomal DNA by in vitro λ packaging (Stratagene, La Jolla, CA). Packaged phage were plated on an SCS-8 bacterial lawn in the presence of 5-bromo-4-chloro-3-indolyl-β-D-galactopyranoside (X-Gal). Phage with a mutated *lacI* gene yield blue plaques, while wild-type phage form colorless plaques. *lacI* mutants were picked and purified by replating at low density. A 1.5-kb *lacI*-containing fragment was amplified by PCR (11), and the mutation specificity was determined by direct sequencing. The MF was calculated as the ratio of the number of independent mutants to the total number of plaques screened. MF data are presented with standard error of the mean (SEM) and were analyzed using COCHARM (created by Troy Johnson, Procter & Gamble, Cincinnati, OH), a computer program that executes the general Cochran-Armitage test (4). Fisher's exact test was used for the comparison of mutation changes, and the Bonferonni correction was used when comparing data from more than two groups.

Chromatid gap/break assay. Spleens were removed from adult mice of all three *p27* genotypes and placed in 1.5 ml of RPMI 1640, and cells were teased out of the spleen using sterile, bent 23-gauge needles. Spleen cell pellets were equally divided into thirds and cultured in T25 flasks with 5 ml RPMI 1640 containing 10% fetal bovine serum (FBS) and 40 μg/ml lipopolysaccharide (Sigma, L4391). Cells were cultured at 37°C for 46 h, followed by treatment with either 0, 0.6, or 1.2 Gy gamma irradiation. After irradiation, cells were incubated for an additional 3 h at 37°C, with the final hour of incubation in the presence of 0.04 μg/ml KaryoMAX Colcemid (Invitrogen). Cells were harvested for metaphase chromosome preparations using 0.075 M KCl (15 min at 37°C), followed by three changes of 3:1 methanol-acetic acid fixative. Slides were prepared and either G banded or solid stained using Wright stain. Fifty to 150 cells from each culture were counted for chromatid gaps and breaks by a blinded scorer and pooled for statistical analysis. Two or three mice per *p27* genotype were analyzed in two separate experiments. Cells were not used for scoring if they had overlapping chromosomes, if debris was covering chromosomes, or if they were tetraploid.

Micronucleus assay. Peripheral blood samples were obtained from seven to nine mice per *p27* genotype by retroorbital bleeding immediately prior to, as well as 24 h and 48 h following, one dose of whole-body 0.6 Gy IR at the age of 8 to 12 weeks. Blood samples were fixed according to the manufacturer's specifications and processed by flow cytometry at Litron Laboratories. The micronucleus frequencies of high $CD71^+$ micronucleated reticulocytes were assayed.

Histopathology and immunohistochemistry. The small intestine and colon were removed, fixed in 10% neutral buffered formalin for 4 to 6 h, and embedded in paraffin. After high-temperature antigen retrieval in 10 mM citrate buffer, pH 6.0, 5-mm sections were stained for p27 (mouse monoclonal antibody; Neomarkers, Fremont, CA), phospho-histone H3 (Ser 10) (Cell Signaling Tech 9701) for 1 h. Standard avidin-biotin peroxidase complex (ABC) techniques were used for primary antibody detection (biotinylated goat anti-rabbit antibody [Vector Labs Inc., Burlingame, CA]; streptavidin ABC [DAKO Corp., Carpinteria, CA]). The slides were developed in 3,3′-diaminobenzidine–NiCl and then counterstained with methyl green. Controls included no primary antibody and/or normal rabbit serum and tissues from $p27^{-/-}$ mice. Bromodeoxyuridine labeling was done as described previously (28).

Cell cycle analysis. To generate mouse embryonic fibroblasts (MEFs), $p27^{+/-}$ mice were crossed and embryos were dissected at 12.5 to 13.5 days after detection of vaginal plugs. The head and internal organs were removed, and the embryos were minced and incubated in 0.05% trypsin for 5 min. The cells were resuspended in Dulbecco modified Eagle medium supplemented with 10% FBS. After

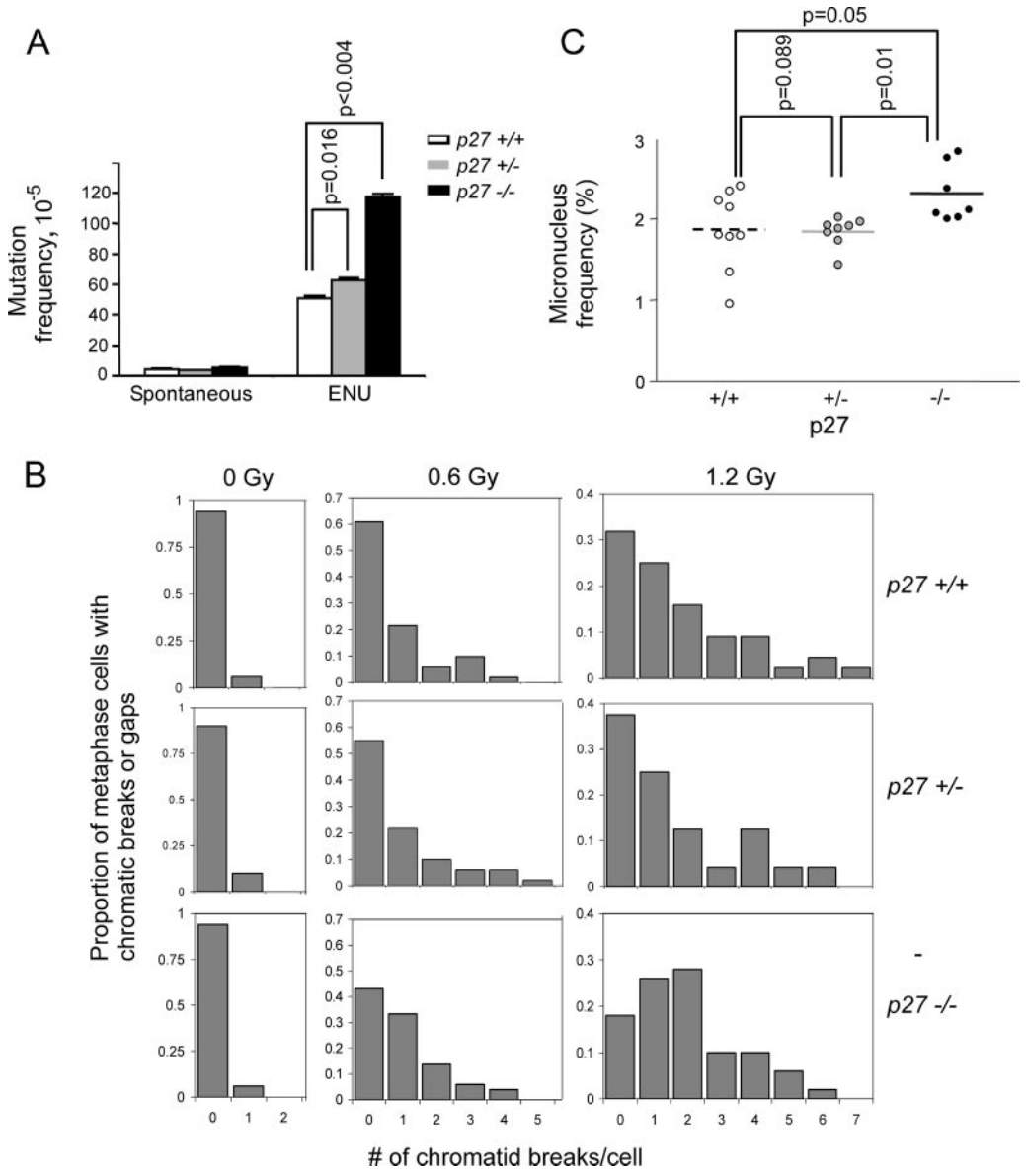

FIG. 1. Increase in DNA damage-induced chromosome damage and mutations in *p27*-deficient mice. (A) Mice of all three *p27* genotypes were analyzed for MF in colonic epithelium of *lacI* transgenic mice following treatment with the point mutagen ENU. $p27^{+/-}$ and $p27^{-/-}$ mice had significantly higher ENU-induced mutation frequencies. Vertical bars represent the SEM. (B) Spleen cultures were prepared from mice of each *p27* genotype. At least 100 metaphase spreads per *p27* genotype were analyzed for chromatid gaps and breaks following gamma irradiation in two independent experiments, one of which is shown. (C) Mice were subjected to retroorbital bleeds before and 48 h following 0.6 Gy gamma irradiation. $p27^{-/-}$ mice have a significantly higher micronucleus frequency in reticulocytes than either $p27^{+/+}$ or $p27^{+/-}$ mice. Horizontal bars indicate the mean frequency of micronucleus formation.

centrifugation, the supernatant was discarded and the cell suspension from each embryo was cultivated on a 10-cm dish in 10 ml Dulbecco modified Eagle medium with 10% FBS until confluence was reached. After this time, the cells were treated with trypsin, counted, and plated at 0.5×10^6 cells per 10-cm dish or at 0.025×10^6 cells per well in a LabtekII chamber slide (Nalge Nunc International). Immortalized MEF lines were prepared according to the NIH 3T3 protocol and were a generous gift from A. Besson and J. Roberts. Adherent primary MEFs were irradiated with 5 Gy at passages 1 to 5, with all p27 genotypes matched for passage within a given experiment. The MI of MEFs was determined using H&E staining of chamber slides in three to five independent experiments. At least three different MEF lines per *p27* genotype were analyzed before and after IR. The results shown are expressed as percentages of the unirradiated MI. For synchronization experiments, cells were grown to confluence and held for 48 h before passage into 5 μg/ml aphidicolin. After 16 h, the cells were washed twice with PBS and released into fresh medium without aphidicolin. For fluorescence-activated cell sorter (FACS) analysis, 0.5×10^6 cells were fixed in 70% ethanol at −20°C for 1 h, washed twice with 2% fetal calf serum–PBS, and stained with 25 μg/ml propidium iodide and 1 mg/ml RNase A in 2% fetal calf serum–PBS overnight at 4°C. Samples were acquired on a FACScan for DNA content and analyzed using Cellquest software (Becton Dickinson, Mountain View, CA) and FlowJo software (TreeStar Inc., Ashland, OR). Fifty percent of cells entered S phase by 4 h after release (see Fig. 4). Therefore, cells were irradiated (5 Gy) at 6 h after release, when a large percentage would be in S/G_2, and then collected 2 h later for mitotic and kinase assays. For analysis of phospho-H2A.X, cells were synchronized as described above and seeded in four-chamber slides at 0.025×10^6 cells per well in a LabtekII chamber slide (Nalge Nunc International). At appropriate time points, cells were fixed with 95% ethanol and 5% acetic acid for 10 min, followed by a

TABLE 2. ENU-induced mutation specificity

Mutation type	$p27^{+/+}$		$p27^{+/-}$		$p27^{-/-}$	
	Mutation % (no./total)[a]	Mean MF ± SEM (10^{-5})[b]	Mutation % (no./total)	Mean MF ± SEM (10^{-5})	Mutation % (no./total)	Mean MF ± SEM (10^{-5})
Transition						
G · C>A · T	30.8 (36/117)	17.0 ± 4.5	33.1 (43/130)	21.2 ± 2.3	26.8 (19/71)	30.5 ± 4.0[c]
A · T>G · C	18.8 (22/117)	7.1 ± 2.5	18.5 (24/130)	10.0 ± 3.0	12.7 (9/71)	16.0 ± 8.0
Transversion						
G · C>T · A	8.5 (10/117)	3.9 ± 1.8	12.3 (16/130)	7.3 ± 2.0	16.9 (12/71)	19.6 ± 2.0[d]
G · C>C · G	0	0	2.3 (3/130)	1.3 ± 0.6	1.4 (1/71)	1.8 ± 0.9
A · T>T · A	30.8 (36/117)	16.2 ± 3.0	23.8 (31/130)	16.0 ± 3.5	26.8 (19/71)	30.6 ± 7.0
A · T>C · G	7.7 (9/117)	2.8 ± 1.4	8.5 (11/130)	5.2 ± 1.4	7.0 (5/71)	8.9 ± 0.4[e]
Other						
+1 frameshifts	0	0	0	0	0	0
−1 frameshifts	1.7 (2/117)	0.6 ± 0.3	0.8 (1/130)	0.8 ± 0.4	7.0 (5/71)	8.2 ± 0.4
Deletion	0	0	0.8 (1/130)	0.8 ± 0.4	0	0
Insertion	0	0	0	0	0	0
Complex changes	1.8 (2/117)	1.2 ± 0.6	0	0	1.4 (1/71)	1.8 ± 0.8

[a] The number of mutants is corrected for potential clonal expansion.
[b] Mutation frequency in each class of mutation.
[c] $P = 0.01$, Fisher's exact test.
[d] $P = 0.001$, Fisher's exact test.
[e] $P = 0.004$, Fisher's exact test.

10-min fixation/permeation with 1% formaldehyde and 0.25% Triton X-100. Slides were blocked in 3% BSA–1× PBS for 30 min at room temperature and then incubated with anti-phospho-H2A.X (ser139)–fluorescein isothiocyanate conjugate (Upstate) according to the manufacturer's specifications overnight at 4°C. Slides were washed five times with PBS and coverslipped with mounting medium containing DAPI (4′,6′-diamidino-2-phenylindole) (Vector Laboratories). Images were visualized using a Nikon E800 and acquired using Metamorph software (Universal Imaging Corp.). The experiment was run in triplicate, and all images for a given experiment were acquired using the same exposure, range, and gamma settings.

Cyclin B1-associated kinase assay. $p27^{+/+}$ and $p27^{-/-}$ immortalized MEFs were lysed in PBS (Sigma, P4417) (pH 7.3), 0.5 mM EDTA, 20 mM EGTA, 15 mM $MgCl_2$, 1 mM dithiothreitol, 2 mM NaF, 1 mM NaVO4, 10% glycerol, 0.5% I-gepal, and 1× protease inhibitors (Roche Complete). Lysates were centrifuged for 45 min at 18,000 × *g* and 4°C, and supernatants were used for kinase assays. Protein concentrations were measured using the Bradford assay (Bio-Rad). Cyclin B1 agarose-conjugated antibody (Santa Cruz, sc-245AC) (5 μg) was incubated with lysates (500 μg) plus BSA at 0.5 mg/ml for 12 h at 4°C. Immunoprecipitated protein complexes [cyclinB1/Cdk1(Cdc2)] were washed twice in lysis buffer and twice in kinase reaction buffer (80 mM β-glycerophosphate [pH 7.3], 20 mM EGTA, 15 mM MgCl2, 10 mM dithiothreitol). For kinase assays, each sample was incubated with 20 μl of kinase reaction buffer, 20 μM ATP, 5 to 10 μCi [γ-^{32}P]ATP (Perkin-Elmer Life Sciences, BLU-502A), and 2.0 μg histone H1 (Roche, 1004875) at 30°C for 30 min. Reactions were terminated by the addition of 10 μl of 4× sodium dodecyl sulfate-polyacrylamide gel electrophoresis sample buffer. Samples were separated on 12% polyacrylamide gels. Phosphorylation was analyzed by autoradiography and quantified by phosphorimager analysis (Molecular Probes, Typhoon Trio).

Immunoblot analysis. Total protein lysates were prepared from primary MEFs using a lysis buffer consisting of 150 mM NaCl, 50 mM Tris [pH 8.0], and 1% NP-40. Protein concentrations were standardized using the Bradford assay (Bio-Rad), and equal loading was confirmed by Ponceau S staining of polyvinylidene difluoride membranes after electroblotting as well as with a loading control (α-tubulin). The antibodies used for immunoblotting were to p27 (N20) and Cdc2 [P34(17)] from Santa Cruz, p21 (rabbit anti-mouse antibody) from BD Pharmingen, p53 Novocastra (CM5), phospho-Chk1 (133D3) and phospho-Cdc2 Thr161 from Cell Signaling, and α-tubulin (clone B-5-1-2) from Sigma. Blots were developed using a chemiluminescence detection kit for horseradish peroxidase (Pierce).

Statistical methods. Two-sample unpaired *t* tests for samples with unequal variance were used for comparison unless otherwise stated. The 95% confidence limits and *P* values are two sided.

RESULTS

Mutations in genotoxin-treated *p27*-deficient mice. Given that p27 functions as a tumor suppressor in multiple epithelial tissues but has no apparent effect on the steady-state proliferative index of adult epithelial tissues (21), we hypothesized that p27 may be important in the cellular response to DNA damage. We therefore investigated the role of p27 in somatic mutagenesis by crossing *p27*-deficient mice to *lacI* transgenic mice (Big Blue mice) and determining the frequency of ENU-induced mutations in the *lacI* gene in colonic epithelium. The use of Big Blue mice in a mammalian mutation assay offers the advantage of determining the in vivo mutagenicity of chemicals in any target organ as well as the ability to identify the specific nature of the induced genetic lesion through recovery and sequencing of the transgene (10). The spontaneous MFs (± SEM) in colons from $p27^{+/+}$, $p27^{+/-}$, and $p27^{-/-}$ mice were similar: $4.3 \times 10^{-5} \pm 0.3 \times 10^{-5}$, $3.8 \times 10^{-5} \pm 0.3 \times 10^{-5}$, and $5.1 \times 10^{-5} \pm 1.0 \times 10^{-5}$, respectively (Table 1). Three weeks after ENU treatment, the MFs increased to $51.0 \times 10^{-5} \pm 3.3 \times 10^{-5}$, $63.0 \times 10^{-5} \pm 2.0 \times 10^{-5}$, and $117.3 \times 10^{-5} \pm 4.7 \times 10^{-5}$ in mice with the three different *p27* genotypes, respectively (Table 1). The ENU-induced MFs in both $p27^{+/-}$ and $p27^{-/-}$ mice were significantly higher than that in $p27^{+/+}$ mice (Fig. 1A) (Cochran-Armitage test), with $p27^{-/-}$ mice demonstrating a greater-than-twofold increase in MF compared to $p27^{+/+}$ mice. The number of cells bearing distinct mutations recovered in these MF assays was significantly higher in *p27*-deficient mice, indicating that clonal expansion after mutation fixation does not explain the increase in the frequency of recovered mutations.

The predominant spontaneous mutations were G · C→A · T transitions and G · C→T · A transversions, regardless of *p27* genotype (data not shown), which is consistent with previous

studies (9). Spontaneous −1 frameshifts were relatively minor in $p27^{+/+}$ mice (3.5%) but accounted for 8.4% and 9.4% in the $p27^{+/-}$ and $p27^{-/-}$ mice, respectively ($P = 0.036$, Fisher's exact test), suggesting that repair in the absence of p27 may rely more heavily on the activity of DNA polymerases that are prone to introducing −1 frameshifts, such as Pol κ, a member of the Y family of translesional DNA polymerases (34). Treatment with ENU altered the mutation spectrum of the colonic epithelium in all *p27* genotypes. ENU induced an increase in the frequency of nearly all types of base substitutions except G · C→C · G transversions, with A · T→T · A substitutions accounting for 30.8% of the spectrum. The frequencies of G · C→A · T, G · C→T · A, and A · T→C · G substitutions in $p27^{-/-}$ mice was significantly higher than that found in wild-type mice (Table 2). $p27^{+/-}$ mice displayed an intermediate phenotype, indicating that p27 is haploinsufficient for the ability to guard against ENU-induced mutation. The frequency of ENU-induced −1 frameshifts remained low in the $p27^{+/+}$ and $p27^{+/-}$ mice ($0.6 \times 10^{-5} \pm 0.3 \times 10^{-5}$ and $0.8 \pm 0.4 \times 10^{-5}$, respectively) but was increased to $8.2 \times 10^{-5} \pm 0.4 \times 10^{-5}$ in $p27^{-/-}$ mice (Table 2), providing further evidence that a distinct repair process favoring −1 frameshifts may occur in $p27^{-/-}$ mice.

Frequency of chromatid gaps and breaks. Chromatid gaps and breaks represent dangerous DNA double-strand breaks that when unrepaired lead to unjoined chromosome elements and if misrepaired may promote breakage-bridge-fusion cycles and continued genetic instability. The frequency of chromatid gaps and breaks is often used as a measure of the cell's ability to repair its DNA or of its ability to arrest prior to entering mitosis. The spontaneous frequencies of chromatid gaps and breaks in lipopolysaccharide-stimulated splenocytes were similar among the *p27* genotypes (Fig. 1B). However, following 0.6 Gy and especially 1.2 Gy gamma irradiation, the frequency of cells containing breaks and the number of breaks per cell were increased in splenocytes from $p27^{-/-}$ mice compared to those from $p27^{+/+}$ mice. $p27^{+/-}$ mice displayed an intermediate response ($P = 0.03$, test for an ordered effect across genotypes).

Frequency of micronucleus formation. The micronucleus assay is a standard test used for the detection of chromosomal damage. It measures the ability of cells to repair DNA damage by detecting the formation of micronuclei (acentric fragments or complete chromosomes that failed to segregate properly and were excluded from the nucleus). Whereas the spleen culture assay involves a short period of in vitro culture prior to assessment of DNA damage, the micronucleus assay directly measures the in vivo response of peripheral blood cells without intermediate culture and thus provides a direct picture of the DNA damage response of cells within the context of the organism. We analyzed micronucleus formation in $p27^{+/+}$, $p27^{+/-}$, and $p27^{-/-}$ mice following low-dose gamma irradiation (high-dose irradiation arrests the majority of reticulocytes and thereby prevents the formation and subsequent recovery of micronuclei). While the spontaneous micronucleus frequencies (mean ± SEM) were similar in the $p27^{+/+}$, $p27^{+/-}$, and $p27^{-/-}$ genotypes (0.30% ± 0.02%, 0.26% ± 0.02%, and 0.29% ± 0.02%, respectively), by 48 h following 0.6 Gy gamma irradiation, it had increased to 1.9% ± 0.16%, 1.8% ± 0.07%, and 2.3% ± 0.13% (Fig. 1C). The micronucleus frequency from $p27^{-/-}$ mice was significantly higher than that from either $p27^{+/-}$ or $p27^{+/+}$ mice.

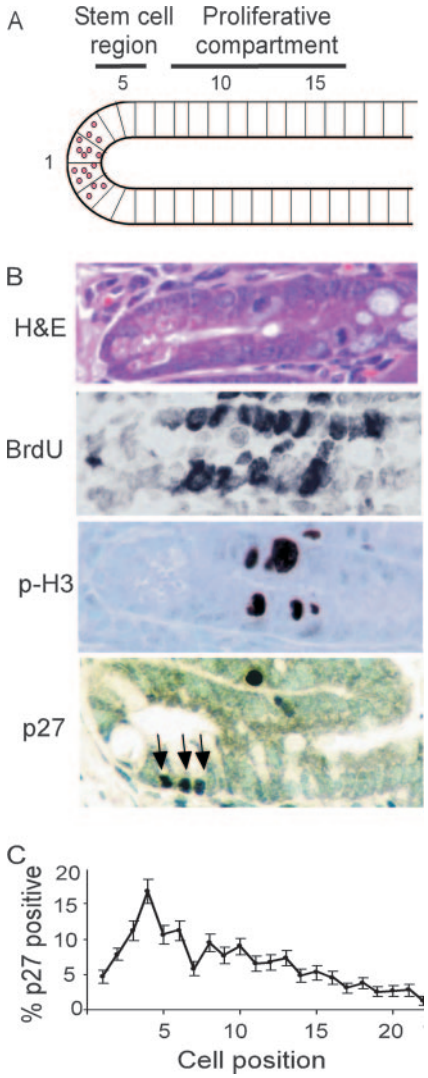

FIG. 2. p27 is expressed in the proliferative compartment of the intestinal crypt (A) Graphic representation of crypt cell position in the small intestine. (B) Representative section of small intestinal crypt stained with H&E and antibodies to bromodeoxyuridine, phosphohistone H3, and p27 (magnification, ×600). Arrows point to p27-positive crypt cells. (C) Distribution of p27-positive staining in the crypt. Error bars indicate SEMs.

p27 is expressed in the proliferative compartment of the intestinal crypt. p27 is a known inhibitor of GI tumorigenesis, and *p27*-deficient colon cells show an increase in MF following genotoxic insult. In order to evaluate the potential target cells of *p27* deficiency in mutagenesis and intestinal tumorigenesis, we assessed the spatial distribution of p27 expression within the intestinal crypts from normal mice. p27-positive cells were found throughout the intestinal crypt; however, the majority were within the bottom 10 cell positions, peaking at cell position four (Fig. 2). Extensive kinetic analysis by Potten and colleagues has shown that the presumptive stem cell of the intestinal crypt resides at or near cell position 4 and that cell positions 5 to 15 contain the transit-amplifying cells, with pro-

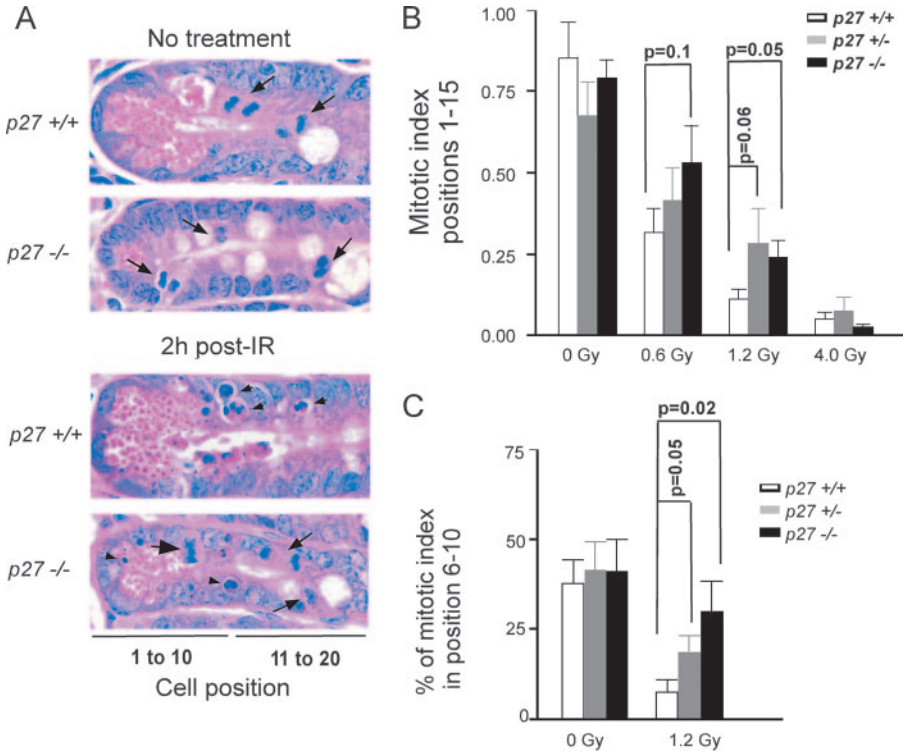

FIG. 3. *p27* deficiency impairs G_2/M arrest in irradiated GI crypt cells. (A) Mitotic cells (arrows) are seen in both $p27^{+/+}$ and $p27^{-/-}$ mice before treatment. Note the reduction of mitotic cells in irradiated $p27^{+/+}$ but not $p27^{-/-}$ crypts. Increased apoptosis is seen in both $p27^{+/+}$ and $p27^{-/-}$ crypts after irradiation (arrowheads) (magnification, ×1,000). (B) $p27^{-/-}$ mice have a significantly higher MI in cell positions 1 to 15 of the SI crypt than $p27^{+/+}$ mice following 1.2 Gy gamma irradiation. $p27^{+/-}$ mice display an intermediate phenotype. (C) $p27^{-/-}$ mice have a significantly higher frequency of mitotic figures in positions 6 to 10 of the SI crypt than $p27^{+/+}$ mice following 1.2 Gy gamma irradiation. Mean mitotic indices plus or minus the SEM are shown.

liferation peaking at cell position 10 (reviewed in reference 1) (Fig. 2B). Thus, p27 expression occurs within the proliferative compartment of the intestinal epithelium.

p27 participates in the G_2/M checkpoint in intestinal crypt cells in response to low-dose gamma irradiation. As p27 is expressed in the GI crypt cells and *p27* deficiency increases MF in the GI, we measured the effect of p27 on cell cycle kinetics in response to a specific genotoxic agent, gamma irradiation. Radiation has been used extensively to study cell kinetics with the intestinal crypt (33). Nakayama et al. demonstrated previously that *p27* deficiency does not impair arrest at the G_1/S checkpoint in response to gamma irradiation (21), and our unpublished results were consistent with this finding. We therefore investigated the role of p27 at the radiation-induced G_2/M checkpoint. $p27^{+/+}$, $p27^{+/-}$, and $p27^{-/-}$ mice were exposed to various doses of gamma irradiation from 0.6 to 4.0 Gy, and the MI of GI crypt cells was assessed.

The MIs within the intestinal crypts from unirradiated mice were similar between *p27* genotypes (Fig. 3B). The *p27* genotype did not alter the apoptotic index at any dose of radiation (data not shown). Radiation-induced G_2/M arrest, however, was impaired in *p27*-deficient mice at low doses (0.6 and 1.2 Gy), although only 1.2 Gy reached statistical significance (Fig. 3). At higher doses (4 Gy), mitosis was equally inhibited in both $p27^{+/+}$ and $p27^{-/-}$ intestinal epithelia, indicating that the effect of p27 is only seen at low doses of irradiation. Radiation-induced cell cycle arrest was most pronounced in cell positions 6 to 10 within the crypt, with an 80% reduction in mitotic figures in wild-type mice ($P = 0.001$) compared to only a 27% reduction in $p27^{-/-}$ mice ($P = 0.39$). The MI in position 6 to 10 from irradiated $p27^{+/+}$ mice was reduced significantly compared to that in $p27^{-/-}$ mice ($P = 0.02$). $p27^{+/-}$ animals again displayed an intermediate phenotype, indicating that even partial loss of p27 impairs G_2/M arrest. Thus, the impaired radiation-induced G_2/M arrest conferred by *p27* deficiency was most pronounced in cell positions 6 to 10, near the peak of p27 expression (Fig. 2).

p27 regulates the G_2/M checkpoint at early time points following gamma irradiation. We further analyzed the impact of *p27* deficiency on the response to gamma irradiation by using primary MEFs. Dose-response studies showed that a dose of 5 Gy resulted in a similar percentage of G_2/M arrest in MEFs as a dose of 1.2 Gy in GI epithelium (data not shown). Whereas mitotic activity in asynchronously growing $p27^{+/+}$ MEFs was reduced by an average of 79% ± 2% at 2 h following 5 Gy, mitotic activity was reduced by only 39% ± 19% in $p27^{-/-}$ cells (Fig. 4A). In order to analyze the role of p27 specifically at the G_2/M boundary, we irradiated synchronized MEFs. Following release from synchronization, $p27^{+/+}$ and $p27^{-/-}$ cells proceed through the cell cycle with similar kinetics (Fig. 4D). $p27^{+/+}$ cells exhibited a pronounced G_2/M arrest as indicated by a reduced MI at 2 h following irradiation (mean of 76% ± 8% reduction in MI), while $p27^{-/-}$ cells exhibited a

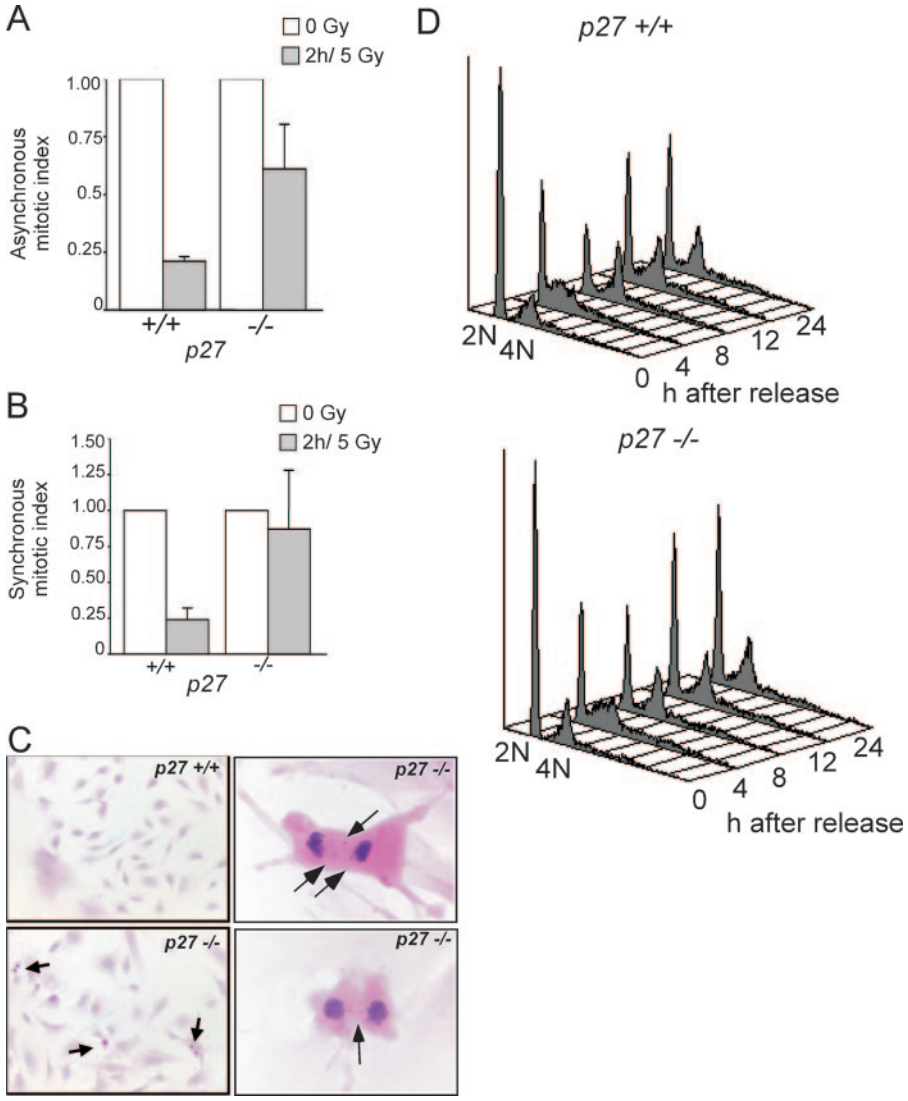

FIG. 4. *p27* deficiency impairs the G_2/M checkpoint in irradiated MEFs. The MI of primary MEFs was determined using H&E-stained chamber slides. The mean MIs plus the SEMs from three to five independent experiments are shown as a percentage of the unirradiated MI. Both asynchronous (A) and synchronous (B) $p27^{-/-}$ MEFs have impaired G_2/M arrest at early time points following low-dose gamma irradiation. (C) H&E-stained chamber slides of MEFs at 2 h following IR. The upper left panel shows a lack of $p27^{+/+}$ mitotic cells due to IR-induced G_2/M arrest (magnification, ×100). The lower left panel shows persistence of $p27^{-/-}$ mitotic cells following IR (magnification, ×100). Arrows indicate mitotic figures. The right panels show aberrant mitotic figures in $p27^{-/-}$ MEFs, including lagging chromosomes and anaphase bridges (arrows) (magnification, ×600). (D) FACS analysis shows that both $p27^{+/+}$ and $p27^{-/-}$ cells were synchronized and proceed into cell cycle after release at similar rates. The data in panel B were from a similar population of cells synchronized at the G_1/S boundary, released, irradiated 6 h later (in late S/G_2), and collected 2 h later.

strongly attenuated G_2/M arrest (mean of 13% ± 41% reduction in MI) (Fig. 4B).

Both $p27^{+/+}$ and $p27^{-/-}$ MEFs displayed a similar increase in the relative number of aberrant mitotic figures per total mitotic cells following gamma irradiation (data not shown). However, due to the higher MI of $p27^{-/-}$ MEFs, the absolute number of aberrant mitotic figures was higher in $p27^{-/-}$ MEFs (53 ± 10 per 10^6 cells) than in $p27^{+/+}$ cells (21 ± 11 per 10^6 cells) (Fig. 4C). Together, these results indicate that a lack of G_2/M arrest directly leads to an increased frequency of aberrant chromosomal segregation, and this is exacerbated in the absence of p27.

As another measure of chromosome damage at early time points following genotoxic damage, we analyzed the kinetics of DNA double-strand break formation in the absence of p27. Phosphorylation of the variant histone H2A.X (also known as gamma-H2A.X) is an early response to DNA double-strand break formation and can be visualized as foci by immunofluorescence (35, 36). Low-dose irradiation of late S/G_2 phase-synchronized MEFs led to a statistically significant increase in phospho-H2A.X staining in $p27^{-/-}$ cells compared to $p27^{+/+}$ cells ($P = 0.009$) by 30 min following exposure, but by 1 h and 2 h following irradiation, the frequencies of phospho-H2A.X positive cells were similar in both $p27^{+/+}$ and $p27^{-/-}$ cells (Fig. 5).

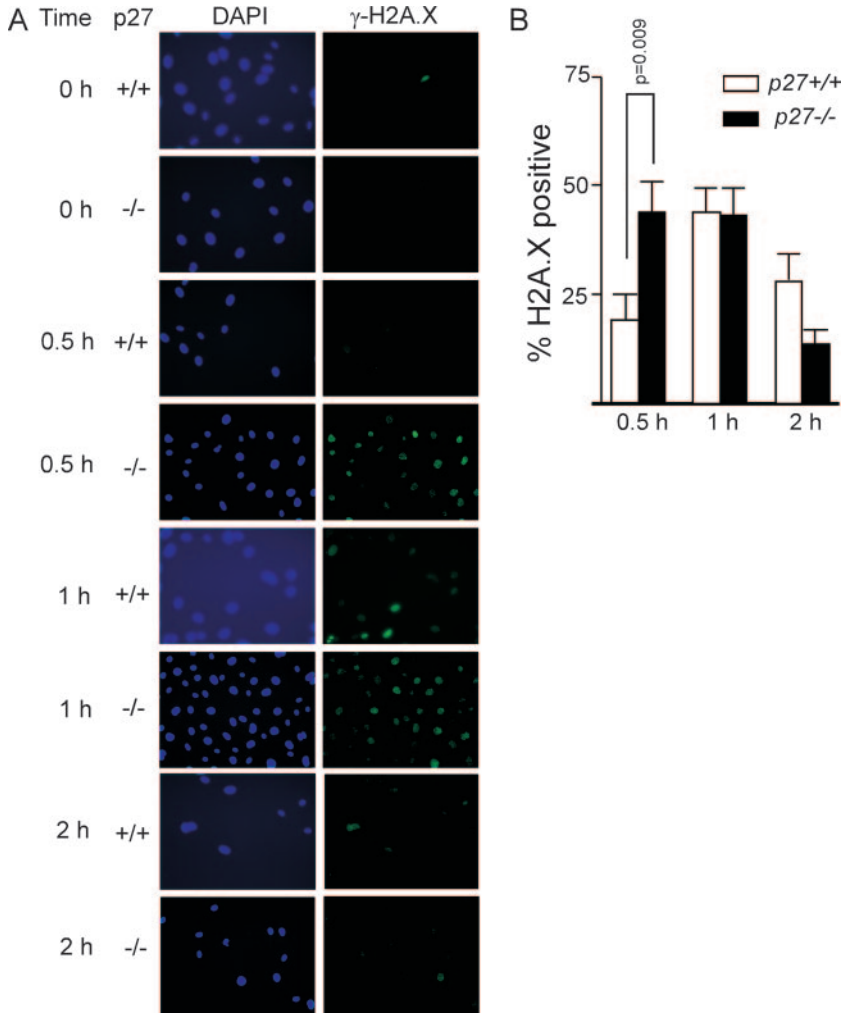

FIG. 5. *p27* deficiency leads to an increase in DNA double-strand breaks at early time points following gamma irradiation. (A) Fluorescence images (magnification, ×200) of representative fields in synchronized primary MEFs harvested at 0 h and at 0.5 h and 1 h following 5 Gy irradiation. All cells are positive for phospho-H2A.X staining by 0.5 h following irradiation; however, the detection threshold was standardized and set to illustrate the difference in signal intensity between $p27^{+/+}$ and $p27^{-/-}$ MEFs. (B) $p27^{-/-}$ MEFs have a higher frequency of phospho-H2A.X positive cells by 30 min following irradiation than $p27^{+/+}$ MEFs ($P = 0.009$). Error bars indicate SEMs.

Mechanism of impaired G_2/M arrest in *p27*-deficient cells. Entry into and progression through mitosis are highly regulated by activation of Cdc2/cyclin B kinase via phosphorylation of Cdc2. Following DNA damage, a signal is transduced via the Chk1 kinase to inhibit Cdc2, leading to G_2/M arrest. Phosphorylation of Chk1 on S345 was seen in both $p27^{+/+}$ and $p27^{-/-}$ cells at 30 min, 1 h, and 2 h after irradiation of synchronized cultures in late S/G_2 (Fig. 6B). p27 itself was not induced at early time points following irradiation (Fig. 6B), while p53 and the Cdk inhibitor p21 were expressed in both $p27^{+/+}$ and $p27^{-/-}$ cells and induced by irradiation by 24 h (data not shown). As checkpoint signaling was intact in the absence of p27, we next examined Cdc2 levels and activity. Synchronized $p27^{-/-}$ cells in late S/G_2 showed higher levels of Cdc2 compared to $p27^{+/+}$ cells both before and after irradiation (Fig. 6B). This increase in Cdc2 was observed only in synchronized MEFs (data not shown). Accordingly, the $p27^{-/-}$ cells also contained higher levels of activated Cdc2 as indicated by phosphorylation on T161 (Fig. 6B). Synchronized wild-type MEFs irradiated in S/G_2 showed the expected inhibition of Cdc2-associated kinase activity especially at 2 to 4 h after IR (Fig. 6C, compare untreated versus 5 Gy panels). In contrast, *p27* null cells showed less inhibition of Cdc2 activity after IR, notably at the 2-h time point. As inhibition of Cdc2 activity is necessary for G_2/M arrest, this explains the impairment of G_2/M arrest in *p27* null cells at early time points following irradiation. This may also explain why impaired arrest in *p27*-deficient cells is apparent only at low doses of IR and at early time points; higher doses or longer times may activate a sufficiently strong response to inhibit the higher levels of Cdc2 seen in $p27^{-/-}$ cells.

***p27* deficiency impairs gamma irradiation-induced G_2/M arrest in autochthonous tumor cells.** As a preliminary investigation into whether the ability of p27 to regulate the cell cycle response to genotoxic damage is related to the prognostic role of p27 in cancer, we analyzed the response of GI adenomas and adenocarcinomas from *Apc* mutant mice to whole-body irradiation based on *p27* genotype. Although radiotherapy is

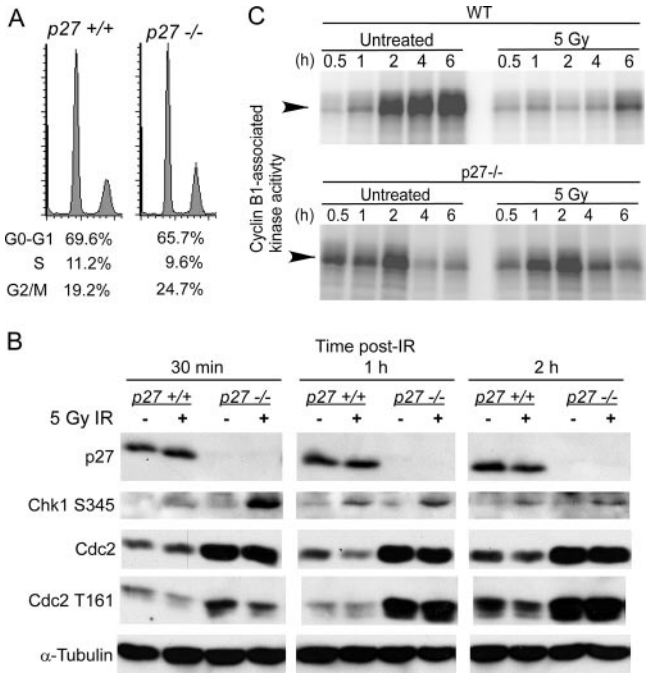

FIG. 6. *p27* deficiency leads to impaired inhibition of Cdc2 in irradiated G_2/M cells. (A) FACS analysis demonstrates efficient synchronization of both $p27^{+/+}$ and $p27^{-/-}$ primary MEFs used for panels B and C. (B) Whole-cell lysates were prepared from synchronized primary MEFs irradiated in late S/G_2, harvested at various times following 5 Gy gamma irradiation, and immunoblotted for the indicated proteins. (C) $p27^{+/+}$ and $p27^{-/-}$ immortalized MEFs were synchronized and then irradiated with 5 Gy in late S/G_2 phase of the cell cycle. At the indicated times, cyclin B1 complexes were immunoprecipitated from cell lysates, and kinase activity toward histone H1 was measured. WT, wild type.

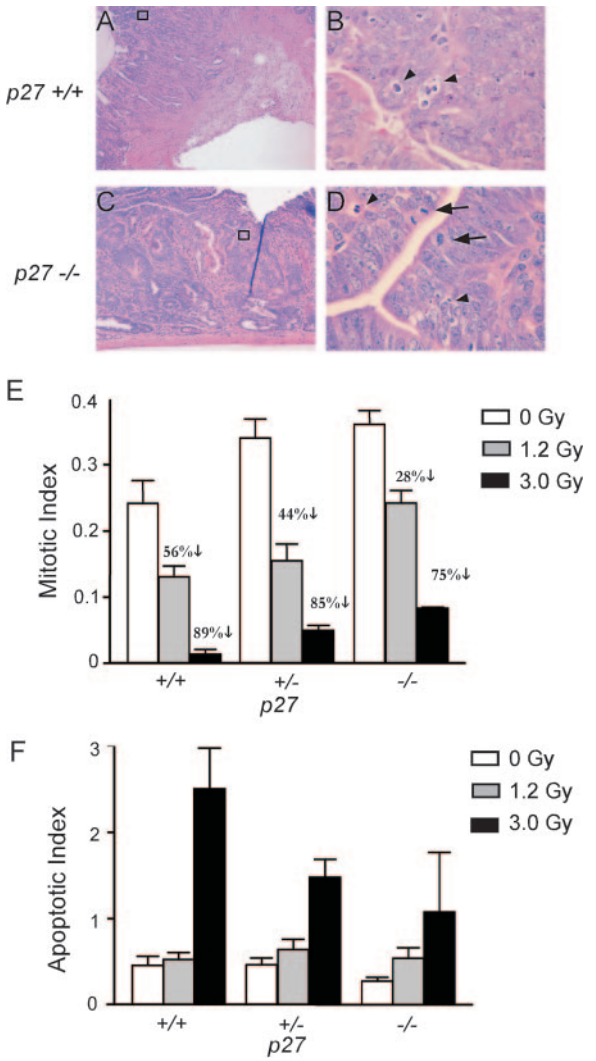

FIG. 7. *p27* deficiency impairs G_2/M arrest in autochthonous tumor cells. *Apc* mutant, $p27^{+/+}$, $p27^{+/-}$, and $p27^{-/-}$ mice bearing intestinal adenomas and adenocarcinomas were irradiated and tumors removed 2 h later. (A to D) H&E-stained sections of $p27^{+/+}$ and $p27^{-/-}$ adenocarcinomas at 2 h following 1.2 Gy (magnifications, ×100 [A and C] and ×1,000 [B and D]). Note persistent mitotic cells (black arrows) in $p27^{-/-}$ compared to $p27^{+/+}$ adenocarcinomas. Arrowheads indicate apoptotic bodies. (E) $p27^{+/+}$ GI tumors have a larger radiation-induced reduction in MI than $p27^{-/-}$ GI tumors. $p27^{-/-}$ GI tumors have a significantly higher MI than $p27^{+/+}$ GI tumors, regardless of irradiation dose (unirradiated, $P = 0.04$; 1.2 Gy, $P = 0.00001$; or 3 Gy, $P = 0.04$). (F) $p27^{+/+}$ GI tumors have a larger, although not statistically significant, radiation-induced increase in apoptotic index than $p27^{-/-}$ GI tumors. Mean indices plus the SEM are shown.

rarely used in human GI cancer, assessment of MI in irradiated tumors is a direct, in vivo measure of the response of these cells to a clinically relevant genotoxic stress. The majority of human colon cancers bear mutations in *APC*, and thus GI tumors from *Apc* mutant mice serve as a relevant preclinical model for therapy response. The MI was significantly greater in GI tumor cells from *p27*-deficient mice, both before ($P = 0.04$) and after whole-body irradiation (1.2 Gy, $P < 0.001$; 3 Gy, $P = 0.04$) (Fig. 7). The MI was reduced by 56% in tumors from irradiated $p27^{+/+}$ mice (1.2 Gy) but by only 44% and 28% in tumors from $p27^{+/-}$ and $p27^{-/-}$ mice, respectively. Thus, *p27* deficiency impaired G_2/M arrest in tumor cells from irradiated mice. This impairment was *p27* gene dosage dependent, indicating that the efficiency of the G_2/M checkpoint in autochthonous tumor cells is markedly sensitive to p27 levels. *p27*-deficient tumor cells also showed impaired apoptotic response to 3 Gy, although this did not reach statistical significance (Fig. 7F).

DISCUSSION

Two mechanisms of tumor suppression by p27. In two models of GI tumorigenesis (chemical induction and germ line *Apc* mutation), we found that p27 functions as a tumor suppressor via inhibition of tumor cell proliferation (28). Here we show that p27 also functions to reduce mutation induction and chromosome damage generated by DNA-damaging agents. *p27* deficiency led to an increased accumulation of point mutations as well as a modest increase in large-scale chromosomal aberrations such as chromatid breaks and micronucleus formation in response to genotoxic stress. The increase in MF in $p27^{-/-}$ mice in the Big Blue mouse assay was comparable to that in other mice with deficiencies of DNA damage response genes, such as *Blm* and *Brca2* (44, 45). Oncogenes are frequently activated by point mutations, and tumor suppressors are frequently inactivated by a variety of mechanisms, from point

mutation to large genomic deletions. Indeed, accumulation of mutations is generally believed to be rate limiting for cancer (19). Reduction of p27 thereby enhances both mitogenesis and mutagenesis on the incipient cancer cell. The observation that loss of p27 increases the frequency of mutations and chromosomal aberrations following genotoxic insult provides an explanation for the sensitivity of *p27*-deficient mice to carcinogens and lends further support for the use of *p27*-deficient mice as a bioassay for carcinogenicity (27). It also suggests that p27 may play a previously unrecognized role in tumor response to genotoxic therapy and subsequent patient survival.

Role of p27 in response to genotoxic damage. Bartek and Lukas (2) have suggested that the cell cycle checkpoint response to DNA damage may occur in two waves, with an initial, transient response occurring within 20 to 30 min and lasting only a few hours, while a second delayed, but more sustained response is mediated by the p53/p21 cascade. In normal, unperturbed intestinal epithelium, p27 is expressed in the proliferative compartment. In contrast, the expression of the related CDK inhibitor p21, while low in unirradiated murine intestinal crypts, is strongly upregulated in a p53-dependent manner by 4 h following gamma irradiation (46). *p27* deficiency affected radiation-induced G_2/M arrest at early (<4 h) but not later time points, suggesting a physiologic role for p27 protein in the immediate response to genotoxic insult, prior to p53-dependent upregulation of p21. The presence of p27 in the GI crypt progenitor cells may function as an immediate-early attenuator for halting cell cycle progression following genotoxic exposure during the time required for p53-dependent transcription and translation of p21 to bring about a sustained cell cycle arrest.

Although other reports have hinted that p27 functions at the G_2/M transition, the physiologic relevance of this role remains unknown (7, 22). Chibazakura et al. found that p27 acts in concert with p21 and p107 to inhibit cyclin A-CDK activity following metaphase (7). Nakayama et al. showed that *Skp2*$^{-/-}$ cells undergo endoreduplication as a result of p27 accumulation in the absence of Skp2-directed proteolysis, indicating that degradation of p27 is required for entry into mitosis (22). Sugihara et al. (40) demonstrated that accumulation of p27 protein at 24 to 48 h following high-dose gamma irradiation is required for suppression of centrosome amplification and prevention of chromosomal instability; however, they did not evaluate either low-dose irradiation or time points earlier than 10 h postirradiation. We observed that p27 protein levels are not altered at early time points following irradiation. Cdc2 levels, however, are higher in G_2/M phase *p27*$^{-/-}$ cells, even in the absence of irradiation, than in *p27*$^{+/+}$ cells. Cdc2 is known to exhibit variation in both RNA and protein levels in addition to the well-characterized posttranslational regulation via inhibitory and activating phosphorylation (17). The mechanism by which p27 might affect Cdc2 protein levels, however, is unclear.

Cdc2 physically interacts with p27 and may be a target of inhibition by p27 (22). We demonstrated that inhibition of Cdc2-associated kinase activity at early time points (<4 h) following IR is impaired in the absence of p27. This agrees with the observation that *p27* deficiency impairs radiation-induced G_2/M arrest at early time points, and taken together, these results provide a plausible mechanism for the increase in the frequency of mutations and chromosomal aberrations following genotoxic insult in *p27*-deficient mice. The delay in G_2/M arrest seen in *p27*$^{-/-}$ cells may be a result of higher levels of Cdc2, which would titrate inhibitory signals, thus necessitating stronger or more sustained DNA damage signaling in order to inhibit its activity and bring about cell cycle arrest. Higher genotoxin doses might elicit stronger cell cycle arrest signals, thus more efficiently inactivating CDKs even in the absence of p27. Thus, p27 functions in the immediate-early DNA damage response to low, more physiologic levels of DNA damage.

Clinical relevance. Radiotherapy for cancer has conventionally been administered as a fractionated dose, i.e., multiple administrations of a low dose of irradiation, in order to minimize the radiosensitivity of proliferating host tissues such as bone marrow and GI epithelium. The relatively recent advent of hyperfractionated radiotherapy attempts to avoid the dose-limiting effects of host radiosensitivity by further reducing the single dose of irradiation while increasing the number of doses administered (reviewed in reference 3). It is clear that intestinal epithelium responds differently depending on the radiation dose and on the molecular background of the target cells (Fig. 3B) (6). In the case of *p27*-deficient cells, they are more likely to continue progression through the cell cycle with concomitant fixation of mutations specifically at the low doses of irradiation that are more likely to be used in cancer therapy. In one of the few studies to examine the response of human tumors of known p27 status to radiotherapy, Oka et al. found that a high p27 labeling index prior to radiotherapy was associated with improved disease-free survival in cervical squamous cell carcinoma patients following a total dose of 27 Gy given in four or five fractionated doses (26), indicating a role for p27 in the response of tumors to fractionated radiotherapy. Further analysis of patient response to radio- or chemotherapy dose based on the p27 status of the tumor warrants investigation.

ACKNOWLEDGMENTS

We thank M. Fero, J. Roberts, and A. Besson for providing *p27* knockout mice and immortalized MEFs and for constructive comments on the manuscript.

This work was supported by the American Cancer Society, the Life Possibilities Fund, and Public Health Service grant CA099517 from the National Cancer Institute. S.R.P. was supported by an NIH training grant in the Molecular Training Program in Cancer Research through the University of Washington.

REFERENCES

1. **Bach, S. P., A. G. Renehan, and C. S. Potten.** 2000. Stem cells: the intestinal stem cell as a paradigm. Carcinogenesis **21:**469–476.
2. **Bartek, J., and J. Lukas.** 2001. Pathways governing G1/S transition and their response to DNA damage. FEBS Lett. **490:**117–122.
3. **Baumann, M., and H. P. Beck-Bornholdt.** 1999. Hyperfractionated radiotherapy: tops or flops? Med. Pediatr. Oncol. **33:**399–402.
4. **Cariello, N. F., and N. J. Gorelick.** 1996. Database and software for the analysis of mutations at the lacI gene in both transgenic rodents and bacteria. Environ. Mol. Mutagen. **28:**397–404.
5. **Catzavelos, C., N. Bhattacharya, Y. C. Ung, J. A. Wilson, L. Roncari, C. Sandhu, P. Shaw, H. Yeger, I. Morava-Protzner, L. Kapusta, E. Franssen, K. I. Pritchard, and J. M. Slingerland.** 1997. Decreased levels of the cell-cycle inhibitor p27Kip1 protein: prognostic implications in primary breast cancer. Nat. Med. **3:**227–230.
6. **Ch'ang, H. J., J. G. Maj, F. Paris, H. R. Xing, J. Zhang, J. P. Truman, C. Cardon-Cardo, A. Haimovitz-Friedman, R. Kolesnick, and Z. Fuks.** 2005. ATM regulates target switching to escalating doses of radiation in the intestines. Nat. Med. **11:**484–490.
7. **Chibazakura, T., S. G. McGrew, J. A. Cooper, H. Yoshikawa, and J. M. Roberts.** 2004. Regulation of cyclin-dependent kinase activity during mitotic exit and maintenance of genome stability by p21, p27, and p107. Proc. Natl. Acad. Sci. USA **101:**4465–4470.

8. **Ciaparrone, M., H. Yamamoto, Y. Yao, A. Sgambato, G. Cattoretti, N. Tomita, T. Monden, H. Rotterdam, and I. B. Weinstein.** 1998. Localization and expression of p27KIP1 in multistage colorectal carcinogenesis. Cancer Res. **58:**114–122.
9. **de Boer, J. G., S. Provost, N. Gorelick, K. Tindall, and B. W. Glickman.** 1998. Spontaneous mutation in lacI transgenic mice: a comparison of tissues. Mutagenesis **13:**109–114.
10. **Dycaico, M. J., G. S. Provost, P. L. Kretz, S. L. Ransom, J. C. Moores, and J. M. Short.** 1994. The use of shuttle vectors for mutation analysis in transgenic mice and rats. Mutat. Res. **307:**461–478.
11. **Erfle, H. L., D. F. Walsh, J. Holcroft, N. Hague, J. G. de Boer, and B. W. Glickman.** 1996. An efficient laboratory protocol for the sequencing of large numbers of lacI mutants recovered from Big Blue transgenic animals. Environ. Mol. Mutagen. **28:**393–396.
12. **Fero, M. L., E. Randel, K. E. Gurley, J. M. Roberts, and C. J. Kemp.** 1998. The murine gene p27Kip1 is haplo-insufficient for tumour suppression. Nature **396:**177–180.
13. **Fero, M. L., M. Rivkin, M. Tasch, P. Porter, C. E. Carow, E. Firpo, K. Polyak, L. H. Tsai, V. Broudy, R. M. Perlmutter, K. Kaushansky, and J. M. Roberts.** 1996. A syndrome of multiorgan hyperplasia with features of gigantism, tumorigenesis, and female sterility in p27-deficient mice. Cell **85:**733–744.
14. **Fodde, R., W. Edelmann, K. Yang, C. van Leeuwen, C. Carlson, B. Renault, C. Breukel, E. Alt, M. Lipkin, and P. M. Khan.** 1994. A targeted chain-termination mutation in the mouse Apc gene results in multiple intestinal tumors. Proc. Natl. Acad. Sci. USA **91:**8969–8973.
15. **Fredersdorf, S., J. Burns, A. M. Milne, G. Packham, L. Fallis, C. E. Gillett, J. A. Royds, D. Peston, P. A. Hall, A. M. Hanby, D. M. Barnes, S. Shousha, M. J. O'Hare, and X. Lu.** 1997. High level expression of p27(kip1) and cyclin D1 in some human breast cancer cells: inverse correlation between the expression of p27(kip1) and degree of malignancy in human breast and colorectal cancers. Proc. Natl. Acad. Sci. USA **94:**6380–6385.
16. **Kawamata, N., R. Morosetti, C. W. Miller, D. Park, K. S. Spirin, T. Nakamaki, S. Takeuchi, Y. Hatta, J. Simpson, and S. Wilcyznski.** 1995. Molecular analysis of the cyclin-dependent kinase inhibitor gene p27/Kip1 in human malignancies. Cancer Res. **55:**2266–2269.
17. **Lee, M. G., C. J. Norbury, N. K. Spurr, P. Nurse, M. G. Lee, C. J. Norbury, N. K. Spurr, and P. Nurse.** 1988. Regulated expression and phosphorylation of a possible mammalian cell-cycle control protein. Nature **333:**676–679.
18. **Loda, M., B. Cukor, S. W. Tam, P. Lavin, M. Fiorentino, G. F. Draetta, J. M. Jessup, and M. Pagano.** 1997. Increased proteasome-dependent degradation of the cyclin-dependent kinase inhibitor p27 in aggressive colorectal carcinomas. Nat. Med. **3:**231–234.
19. **Loeb, L. A.** 1991. Mutator phenotype may be required for multistage carcinogenesis. Cancer Res. **51:**3075–3079.
20. **Mori, M., K. Mimori, T. Shiraishi, S. Tanaka, H. Ueo, K. Sugimachi, and T. Akiyoshi.** 1997. p27 expression and gastric carcinoma. Nat. Med. **3:**593.
21. **Nakayama, K., N. Ishida, M. Shirane, A. Inomata, T. Inoue, N. Shishido, I. Horii, and D. Loh.** 1996. Mice lacking p27 display increased body size, multiple organ hyperplasia, retinal dysplasia, and pituitary tumors. Cell **85:**707–720.
22. **Nakayama, K., H. Nagahama, Y. A. Minamishima, S. Miyake, N. Ishida, S. Hatakeyama, M. Kitagawa, S. Iemura, T. Natsume, and K. I. Nakayama.** 2004. Skp2-mediated degradation of p27 regulates progression into mitosis. Dev. Cell **6:**661–672.
23. **Nishino, H., A. Knoll, V. L. Buettner, C. S. Frisk, Y. Maruta, J. Haavik, and S. S. Sommer.** 1995. p53 wild-type and p53 nullizygous Big Blue transgenic mice have similar frequencies and patterns of observed mutation in liver, spleen and brain. Oncogene **11:**263–270.
24. **Noguchi, T., R. Kikuchi, K. Ono, S. Takeno, H. Moriyama, and Y. Uchida.** 2003. Prognostic significance of p27/kip1 and apoptosis in patients with colorectal carcinoma. Oncol. Rep. **10:**827–831.
25. **Ohtani, M., H. Isozaki, K. Fujii, E. Nomura, M. Niki, H. Mabuchi, K. Nishiguchi, M. Toyoda, T. Ishibashi, and N. Tanigawa.** 1999. Impact of the expression of cyclin-dependent kinase inhibitor p27Kip1 and apoptosis in tumor cells on the overall survival of patients with non-early stage gastric carcinoma. Cancer **85:**1711–1718.
26. **Oka, K., Y. Suzuki, and T. Nakano.** 2000. Expression of p27 and p53 in cervical squamous cell carcinoma patients treated with radiotherapy alone: radiotherapeutic effect and prognosis. Cancer **88:**2766–2773.
27. **Payne, S. R., and C. J. Kemp.** 2003. p27(Kip1) (Cdkn1b)-deficient mice are susceptible to chemical carcinogenesis and may be a useful model for carcinogen screening. Toxicol. Pathol. **31:**355–363.
28. **Philipp-Staheli, J., K. H. Kim, S. R. Payne, K. E. Gurley, D. Liggitt, G. Longton, and C. J. Kemp.** 2002. Pathway-specific tumor suppression. Reduction of p27 accelerates gastrointestinal tumorigenesis in Apc mutant mice, but not in Smad3 mutant mice. Cancer Cell **1:**355–368.
29. **Philipp-Staheli, J., S. R. Payne, and C. J. Kemp.** 2001. p27(Kip1): regulation and function of a haploinsufficient tumor suppressor and its misregulation in cancer. Exp. Cell Res. **264:**148–168.
30. **Pietenpol, J. A., S. K. Bohlander, Y. Sato, N. Papadopoulos, B. Liu, C. Friedman, B. J. Trask, J. M. Roberts, K. W. Kinzler, J. D. Rowley, et al.** 1995. Assignment of the human p27Kip1 gene to 12p13 and its analysis in leukemias. Cancer Res. **55:**1206–1210.
31. **Ponce-Castaneda, M. V., M. H. Lee, E. Latres, K. Polyak, L. Lacombe, K. Montgomery, S. Mathew, K. Krauter, J. Sheinfeld, J. Massague, et al.** 1995. p27Kip1: chromosomal mapping to 12p12-12p13.1 and absence of mutations in human tumors. Cancer Res. **55:**1211–1214.
32. **Porter, P. L., K. E. Malone, P. J. Heagerty, G. M. Alexander, L. A. Gatti, E. J. Firpo, J. R. Daling, and J. M. Roberts.** 1997. Expression of cell-cycle regulators p27 Kip-1 and cyclin E alone and in combination, correlate with survival in young breast cancer patients. Nat. Med. **3:**222–225.
33. **Potten, C. S.** 2004. Radiation, the ideal cytotoxic agent for studying the cell biology of tissues such as the small intestine. Radiat. Res. **161:**123–136.
34. **Prakash, S., R. E. Johnson, L. Prakash, S. Prakash, R. E. Johnson, and L. Prakash.** 2005. Eukaryotic translesion synthesis DNA polymerases: specificity of structure and function. Annu. Rev. Biochem. **74:**317–353.
35. **Rogakou, E. P., C. Boon, C. Redon, and W. M. Bonner.** 1999. Megabase chromatin domains involved in DNA double-strand breaks in vivo. J. Cell Biol. **146:**905–916.
36. **Rogakou, E. P., D. R. Pilch, A. H. Orr, V. S. Ivanova, and W. M. Bonner.** 1998. DNA double-stranded breaks induce histone H2AX phosphorylation on serine 139. J. Biol. Chem. **273:**5858–5868.
37. **Sgambato, A., C. Ratto, B. Faraglia, M. Merico, R. Ardito, G. Schinzari, G. Romano, and A. R. Cittadini.** 1999. Reduced expression and altered subcellular localization of the cyclin-dependent kinase inhibitor p27(Kip1) in human colon cancer. Mol. Carcinog. **26:**172–179.
38. **Shamma, A., Y. Doki, T. Tsujinaka, H. Shiozaki, M. Inoue, M. Yano, K. Kawanishi, and M. Monden.** 2000. Loss of p27(KIP1) expression predicts poor prognosis in patients with esophageal squamous cell carcinoma. Oncology **58:**152–158.
39. **Singh, S. P., J. Lipman, H. Goldman, F. H. Ellis, Jr., L. Aizenman, M. G. Cangi, S. Signoretti, D. S. Chiaur, M. Pagano, and M. Loda.** 1998. Loss or altered subcellular localization of p27 in Barrett's associated adenocarcinoma. Cancer Res. **58:**1730–1735.
40. **Sugihara, E., M. Kanai, S. Saito, T. Nitta, H. Toyoshima, K. Nakayama, K. I. Nakayama, K. Fukasawa, M. Schwab, H. Saya, and M. Miwa.** 2006. Suppression of centrosome amplification after DNA damage depends on p27 accumulation. Cancer Res. **66:**4020–4029.
41. **Suri, A., J. deBoer, W. Kusser, and B. W. Glickman.** 1996. A 3 milliTesla 60 Hz magnetic field is neither mutagenic nor co-mutagenic in the presence of menadione and MNU in a transgenic rat cell line. Mutat. Res. **372:**23–31.
42. **Thomas, G. V., K. Szigeti, M. Murphy, G. Draetta, M. Pagano, and M. Loda.** 1998. Down-regulation of p27 is associated with development of colorectal adenocarcinoma metastases. Am. J. Pathol. **153:**681–687.
43. **Tsihlias, J., L. Kapusta, and J. Slingerland.** 1999. The prognostic significance of altered cyclin-dependent kinase inhibitors in human cancer. Annu. Rev. Med. **50:**401–423.
44. **Tutt, A. N., C. T. van Oostrom, G. M. Ross, H. van Steeg, and A. Ashworth.** 2002. Disruption of Brca2 increases the spontaneous mutation rate in vivo: synergism with ionizing radiation. EMBO Rep. **3:**255–260.
45. **Wang, Y., and J. A. Heddle.** 2004. Spontaneous and induced chromosomal damage and mutations in Bloom syndrome mice. Mutat. Res. **554:**131–137.
46. **Wilson, J. W., D. M. Pritchard, J. A. Hickman, and C. S. Potten.** 1998. Radiation-induced p53 and p21WAF-1/CIP1 expression in the murine intestinal epithelium: apoptosis and cell cycle arrest. Am. J. Pathol. **153:**899–909.
47. **Yang, W., L. Bancroft, J. Liang, M. Zhuang, and L. H. Augenlicht.** 2005. p27kip1 in intestinal tumorigenesis and chemoprevention in the mouse. Cancer Res. **65:**9363–9368.
48. **Yasui, W., Y. Kudo, S. Semba, H. Yokozaki, and E. Tahara.** 1997. Reduced expression of cyclin-dependent kinase inhibitor p27Kip1 is associated with advanced stage and invasiveness of gastric carcinomas. Jpn. J. Cancer Res. **88:**625–629.